Complementary Intersection Method for System Reliability Analysis

Byeng D. Youn
e-mail: bdyoun@umd.edu

Pingfeng Wang
e-mail: pfwang@umd.edu

University of Maryland,
College Park, MD 20742

Although researchers desire to evaluate system reliability accurately and efficiently over the years, little progress has been made on system reliability analysis. Up to now, bound methods for system reliability prediction have been dominant. However, two primary challenges are as follows: (1) Most numerical methods cannot effectively evaluate the probabilities of the second (or higher)–order joint failure events with high efficiency and accuracy, which are needed for system reliability evaluation and (2) there is no unique system reliability approximation formula, which can be evaluated efficiently with commonly used reliability methods. Thus, this paper proposes the complementary intersection (CI) event, which enables us to develop the complementary intersection method (CIM) for system reliability analysis. The CIM expresses the system reliability in terms of the probabilities of the CI events and allows the use of commonly used reliability methods for evaluating the probabilities of the second–order (or higher) joint failure events efficiently. To facilitate system reliability analysis for large-scale systems, the CI-matrix can be built to store the probabilities of the first- and second-order CI events. In this paper, three different numerical solvers for reliability analysis will be used to construct the CI-matrix numerically: first-order reliability method, second-order reliability method, and eigenvector dimension reduction (EDR) method. Three examples will be employed to demonstrate that the CIM with the EDR method outperforms other methods for system reliability analysis in terms of efficiency and accuracy. [DOI: 10.1115/1.3086794]

1 Introduction

In the past few decades, the importance of reliability has been well conceived by engineers, and considerable advances have been made in reliability-based design optimization (RBDO) [1–4]. Moreover, new methods for reliability assessment have been proposed to enhance numerical efficiency and stability [5–9]. Reliability is defined as a chance that system performance (e.g., fatigue, corrosion, and fracture) meets its marginal value during a system life. Compared with tremendous advances in component reliability analysis and design optimization, the research in system reliability analysis has been stagnant, mainly due to two technical difficulties. First, it is hard to formulate system reliability explicitly for a given system redundancy. Second, even if system reliability is given explicitly, most numerical methods cannot effectively assess system reliability with high efficiency and accuracy. Since system reliability prediction is significantly important in aerospace, mechanical, and civil engineering fields, its technical development will have an immediate and major impact on complex engineering system designs.

Due to the difficulties, system reliability analysis provides the bounds of system reliability, instead of its unique value. The first-order bound methods for serial system reliability and parallel system reliability were proposed in 1960s and 1980s by Ang and other researchers [10,11]. Basically, these methods give an upper system reliability bound by assuming that all system failure events are perfectly dependent; similarly a lower system reliability bound is obtained by assuming that all system failure events are mutually exclusive. The application of these first-order bound methods is limited since they usually give quite wide bounds. Later, Ditlevsen and Bjerager [13] proposed the most widely used second-order system reliability bound method, which gives much tighter bounds than the first-order bounds for both serial and parallel systems. Other equivalent forms of Ditlevsen's bounds are given by Thoft-Christensen and Murotsu [14], Karamchandani [15], Xiao and Mahadevan [16], and Ramachandran [17]. Recently, Song and Der Kiureghian [18] formulated system reliability to a linear programming (LP) problem, referred to as the LP bound method. The LP bound method is able to calculate the optimal bounds for system reliability based on available information. However, it is known that the LP bound method can suffer when an approximate LP algorithm is used for overconstrained problems. Besides, it is extremely sensitive to the accuracy of the given input information, which are the probabilities for the first-, second-, and high-order joint safety events. To ensure high accuracy of the LP bound method, the input probabilities must be given very accurately and the problem must not be overconstrained. Advanced system reliability bound methods (the second-order reliability bound method and LP bound method) provide piecewise continuous system reliability with respect to design variables. In order to carry out system RBDO using these bound methods, response surfaces have to be created for reliability bounds. Additional literatures on system RBDO can be found in Refs. [19–22].

Besides the system reliability bound methods, one of the popular approaches is the multimodal adaptive importance sampling (AIS) method, which is found to be satisfactory for the system reliability analysis of large structures [23,24]. The integration of surrogate model techniques with Monte Carlo simulation (MCS)–based methods can be an alternative approach to system reliability prediction as well [25]. In this approach, the surrogate model can be constructed for multiple limit state functions to represent the joint failure region. This approach is quite practical and highly valued, but accuracy of the method depends on the fidelity of the surrogate model and the number of random input variables.

Although most numerical methods cannot evaluate the probabilities of the second- or higher-order joint safety events with

Contributed by the Design Automation Committee of ASME for publication in the JOURNAL OF MECHANICAL DESIGN. Manuscript received March 18, 2008; final manuscript received January 7, 2009; published online March 20, 2009. Review conducted by Zissimos P. Mourelatos. Paper presented at the ASME 2007 Design Engineering Technical Conferences and Computers and Information in Engineering Conference (DETC2007), Las Vegas, NV, September 4–7, 2007.

high efficiency and accuracy, various reliability analysis methods have been developed and considered for system reliability analysis. These methods mainly fall into four different categories: (1) sampling methods [26–30], (2) expansion methods [31–34], (3) most probable point (MPP)–based methods [35–38], and (4) approximate integration methods [39–42]. Sampling methods, such as MCS and adaptive importance sampling, are quite accurate but inefficient. The expansion methods (e.g., perturbation method) and MPP-based methods (e.g., first-order reliability method (FORM) and second-order reliability method (SORM)) are moderately accurate and efficient. The approximate integration methods, such as the eigenvector dimension reduction (EDR) [9] method, are found to be quite accurate and efficient for reliability analysis.

The primary challenge in system reliability assessment lies in efficient and accurate determination of the probabilities of joint safety events, which are defined as $E_i \cap E_j = \{X | G_i \leq 0 \cap G_j \leq 0\}$. To resolve this challenge, this paper presents a new method for system reliability analysis, referred to as the complementary intersection method (CIM). The complementary intersection (CI) event is defined for the proposed CIM. Then, the probability of the joint safety event can be decomposed in terms of the probabilities of the CI events. This decomposition enables the use of any reliability analysis method for evaluating the probabilities of the second- or higher-order joint safety events. For large-scale systems, the probabilities of the CI events can be conveniently written in the CI-matrix. In this paper, three different reliability methods will be used to construct the CI-matrix numerically: FORM, SORM, and the EDR method. Although stochastic expansion (SE) method [43] is not used in this paper, it can be a good candidate for reliability analysis. But an exhaustive investigation of all those numerical methods is beyond the scope of this study. Instead, this paper mainly focuses on the CIM for system reliability assessment. Section 2 gives a brief review of reliability methods: FORM, SORM, and the EDR method for construction of the CI-matrix. The proposed CIM for system reliability assessment will be presented in Sec. 3. In Sec. 4, three examples are used to demonstrate the effectiveness of the proposed CIM for system reliability analysis. Consequently, it is shown that the CIM can assess system reliability accurately and efficiently, so it can be used for system RBDO.

2 A Review of Reliability Methods for Component Reliability Analysis

An engineering system generally consists of numerous failure modes. Before the system is analyzed, all individual failure modes and their coupled effects must be carefully analyzed. All engineering (say, mechanical) parts in a system are designed to fulfill multiple missions. A failure is thus defined as a nonfulfillment of one of the missions. Each failure mode has a corresponding limit state, which separates the design space into failure and safe regions. The probability of failure, P_f, is denoted as

$$P_f = P(G(\mathbf{X}) > 0) \tag{1}$$

where $G(\mathbf{X})$ is the performance function and $\mathbf{X}$ is the random vector. The limit state is denoted by the equation $G(\mathbf{X})=0$. An exact solution of P_f can be obtained by the multidimensional integration of the joint probability density function (PDF), $f_{\mathbf{X}}(\mathbf{x})$, over the failure domain, $G(\mathbf{X})>0$, which is denoted as

$$P_f = \int_{G(X)>0} \cdots \int f_{\mathbf{X}}(\mathbf{x}) d\mathbf{x} \tag{2}$$

It is very difficult to conduct a multidimensional integration over the implicit failure domain in Eq. (2). Therefore, different approaches (see Sec. 1) have been developed to evaluate the probability of the failure in Eq. (2). Considering numerical accuracy and efficiency, the MPP-based methods and the EDR method will be reviewed in the following sections.

2.1 Most Probable Point–Based Approaches. Through a linear approximation of the failure surface, reliability can be defined as a rotationally invariant measure (a distance from the origin to the MPP): the FORM and the SORM. The MPP is the point having the minimum distance from the origin to the limit state surface. The distance is then defined as a reliability index, β. This reliability analysis method requires a transformation $\mathbf{T}$ from the original random parameter $\mathbf{X}$ to the independent and standard normal random parameter $\mathbf{U}$. Then, the first-order estimate of the failure probability is

$$P_f = \Phi(-\beta) \tag{3}$$

where Φ is the standard normal distribution function. This is referred to as the FORM.

Similarly, the failure probability can be calculated with the second-order approximation of the failure surface

$$P_f = \Phi(-\beta) \prod_{i=1}^{n-1} (1 + \beta\kappa_i)^{-1/2} \tag{4}$$

where the κ_i denotes the principal curvatures of the limit state at the MPP and n is the total number of random variables. This is called the SORM. In both FORM and SORM, the reliability index β can be obtained by solving an optimization problem with one equality constraint [36,37].

2.2 Eigenvector Dimension Reduction Method. The EDR method [9] approximates the statistical moments (e.g., mean, standard deviation, skewness, and kurtosis) of a system performance, its PDF, and reliability. In general, statistical moments of system responses can be calculated as

$$E\{Y^m(\mathbf{X})\} = \int_{-\infty}^{+\infty} \cdots \int_{-\infty}^{+\infty} Y^m(\mathbf{x}) \cdot f_{\mathbf{X}}(\mathbf{x}) \cdot d\mathbf{x} \tag{5}$$

In Eq. (5) a major challenge is a multidimensional integration over the entire random input domain. To resolve this difficulty, the EDR method uses an additive decomposition [8,9,41] that converts a multidimensional integration in Eq. (5) into multiple one-dimensional integrations. Thus, Eq. (5) can be approximated as

$$E[Y^m(\mathbf{X})] \simeq E[\bar{Y}^m(\mathbf{X})] = \int_{-\infty}^{\infty} \cdots \int_{-\infty}^{\infty} \bar{Y}^m \cdot f_{\mathbf{X}}(\mathbf{x}) \cdot d\mathbf{x} \tag{6}$$

where $\bar{Y} = \Sigma_{j=1}^{N} Y(\mu_1, \ldots, \mu_{j-1}, X_j, \mu_{j+1}, \ldots, \mu_n) - (n-1) \cdot Y(\mu_1, \ldots, \mu_n)$. Using a binomial formula, Eq. (6) can be evaluated by executing one-dimensional integration recursively. Uncertainty of the system performance can be evaluated through multiple one-dimensional numerical integrations. The challenge of the problem still remains how to carry out one-dimensional integration effectively. To overcome the challenge, the EDR method incorporates three technical components: (1) eigenvector sampling, (2) one-dimensional response approximation for effective numerical integration, and (3) a stabilized Pearson system for PDF generation.

2.2.1 Eigenvector Sampling. Accuracy in probability analysis can be increased as the number of integration points increases in recursive one-dimensional integrations. However, the increase in integration points makes probability analysis prohibitively expensive. To achieve both accuracy and efficiency in probability analysis, a one-dimensional response surface can be created using samples along the eigenvectors. The eigenvectors are obtained from the covariance matrix of the random input variables. For uncorrelated random variables, the original random axes become the eigenvectors. Otherwise, the eigenvectors will be obtained from the covariance matrix. For efficiency, the EDR method employs only either three or five samples along each eigenvector,

depending on nonlinearity of the system responses. For n number of random parameters, the EDR method demands $2n+1$ or $4n+1$ samples including the design point.

2.2.2 Stepwise Moving Least-Squares Method for Numerical Integration. The moving least-squares (MLS) method [44] is integrated with a stepwise regression method [45], referred to as the stepwise moving least-squares (SMLS) method. The optimal set of basis terms is adaptively chosen to maximize numerical accuracy in the approximate response surface by screening the importance of basis terms. The SMLS method allows the increase in the number of numerical integration points without requiring actual evaluations of system performances through simulations or experiments. Thus, a large number of integration points can be used to increase numerical accuracy in assessing statistical moments of the responses while maintaining high efficiency. There is no restriction to choose numerical integration schemes.

2.2.3 A Stabilized Pearson System. The Pearson system [46] can be used to construct the PDF of a random response (Y) using the first four statistical moments (mean, standard deviation, skewness, and kurtosis). A singularity problem is often found while calculating the coefficients of a specific distribution type. In the EDR method, a stabilized Pearson system is proposed to avoid instability by generating two hyper-PDFs. The hyper-PDFs are employed when the Pearson system fails to build the PDF for a given set of statistical moments of system response. The hyper-PDFs can be constructed using the Pearson system with a tiny perturbation of kurtosis (the fourth moment) value. These two hyper-PDFs are finally used to approximate the PDF with the original statistical moments. More information can be found in Ref. [9]. The EDR method will be employed in this paper as a numerical solver of the proposed CIM.

3 CIM for System Reliability Analysis

This section presents the proposed CIM. Section 3.1 proposes the first-ever defined event, referred to as the CI event, which facilitates the decomposition of the probability of the joint safety event. First, the general formula for the decomposition of the probability of joint safety events will be proposed. As a numerical showcase, the probability of the second-order joint safety event will be introduced and decomposed into the probabilities of the CI events. In order to deal with large-scale problems, Sec. 3.2 introduces the CI-matrix that is composed of the probabilities of the first- and second-order CI events. Section 3.3 proposes an explicit formula of system reliability, which can be used for system RBDO.

3.1 CI Event and Probability Decomposition Theorem. This section proposes the first-ever defined event, referred to as the CI event. This event enables the decomposition of the probability of any second- or higher-order events into the probabilities of the CI events.

3.1.1 Definition: Complementary Intersection Event. Let an Nth-order CI event denote $E_{12,\cdots,N} \equiv \{X | G_1 \cdot G_2 \cdot \cdots \cdot G_N \leq 0\}$, where the component safety (or first-order CI) event is defined as $E_i = \{X | G_i \leq 0, i = 1, 2, \ldots, N\}$. The defined Nth-order CI event is actually composed of N distinct intersections of component events E_i and their complements $\bar{E}_j$ in total where $i = 1, \ldots, N$, $j = 1, \ldots, N$, $i \neq j$. For example, for the second-order CI event E_{ij}, it is composed of two distinct intersection events, $\bar{E}_1 E_2$ and $E_1 \bar{E}_2$. These two events are the intersections of E_1 (or E_2) and the complementary event of E_2 (or E_1). Thus, we refer to the defined event as the CI event.

3.1.2 Theorem: Decomposition of the Probability of an N-th-Order Joint Safety Event. With the definition of the CI event, the probability of an Nth-order joint safety event can be decomposed into the probabilities of the CI events as

$$P\left(\bigcap_{i=1}^{N} E_i\right) = \frac{1}{2^{N-1}}\left[\sum_{i=1}^{N} P(E_i) - \sum_{\substack{i=1 \\ j=2 \\ i<j}}^{N} P(E_{ij}) + \sum_{\substack{i=1 \\ j=2 \\ k=3 \\ i<j<k}}^{N} P(E_{ijk}) + \cdots + (-1)^{m-1} \sum_{\substack{i=1 \\ j=2 \\ \vdots \\ l=m \\ i<j<\cdots<l}}^{N} P(\underbrace{E_{ij\ldots l}}_{m}) + \cdots + (-1)^{N-1} P(E_{12\cdots N})\right] \tag{7}$$

The detailed derivation of Eq. (7) can be found in Appendix A. It is noted that each CI event has its own limit state function, which enables the use of any reliability analysis methods. In general, higher-order CI events are expected to be highly nonlinear. Considering the tradeoff between computational efficiency and accuracy, this paper uses the probabilities of the first- and second-order CI events in Eq. (7) for system reliability analysis. However, more terms in Eq. (7) can be employed as advanced reliability analysis methods are developed in the future.

Based on the definition of the CI event, the second-order CI event can be denoted as $E_{ij} \equiv \{X | G_i \cdot G_j \leq 0\}$. The CI event can be further expressed as $E_{ij} = \bar{E}_i E_j \cup E_i \bar{E}_j$ where the component failure events are defined as $\bar{E}_i = \{X | G_i > 0\}$ and $\bar{E}_j = \{X | G_j > 0\}$. The event E_{ij} is composed of two events: $E_i \bar{E}_j = \{X | G_i \leq 0 \cap G_j > 0\}$ and $\bar{E}_i E_j = \{X | G_i > 0 \cap G_j \leq 0\}$. Since the events, $\bar{E}_i E_j$ and $E_i \bar{E}_j$, are disjoint, the probability of the CI event E_{ij} can be expressed as

$$\begin{aligned} P(E_{ij}) &\equiv P(X | G_i \cdot G_j \leq 0) \\ &= P(X | G_i > 0 \cap G_j \leq 0) + P(X | G_i \leq 0 \cap G_j > 0) \\ &= P(\bar{E}_i E_j) + P(E_i \bar{E}_j) \end{aligned} \tag{8}$$

Based on the probability theory, the probability of the second-order joint safety event $E_i \cap E_j$ can be expressed as

$$P(E_i E_j) = P(E_i) - P(E_i \bar{E}_j) = P(E_j) - P(\bar{E}_i E_j) \tag{9}$$

From Eqs. (8) and (9), the probabilities of the second-order joint safety and failure events can be decomposed as

$$P(E_i E_j) = \tfrac{1}{2}[P(E_i) + P(E_j) - P(E_{ij})] \tag{10}$$

$$P(\bar{E}_i \bar{E}_j) = 1 - \tfrac{1}{2}[P(E_i) + P(E_j) + P(E_{ij})] \tag{11}$$

Figure 1 graphically illustrates the CI event E_{12} in the two shaded domains, $E_{12} = \{(X_1, X_2) | G_1 \cdot G_2 \leq 0\}$. Two component

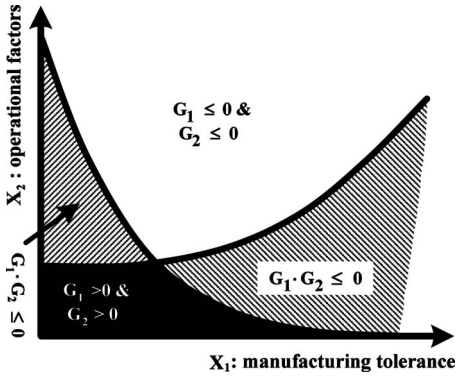

Fig. 1 Definition of the CI event E_{12}

safety events are defined as $E_1=\{(X_1,X_2)|G_1\leq 0\}$ and $E_2=\{(X_1,X_2)|G_2\leq 0\}$, where X_1 and X_2 are random variables (e.g., random manufacturing tolerances and operational conditions).

Although the idea of the CI event and the decomposition theorem can be applicable to series, parallel, and mixed systems with arbitrary system redundancy, only series systems are considered in this paper.

One example is used to demonstrate the procedure of calculating the probability of a second-order joint safe event. Also, FORM. SORM, EDR method, and MCS are used for comparison purposes. In this example, two nonlinear functions $G_1=1-X_1^2X_2/20$ and $G_2=1-(X_1+X_2-5)^2/30-(X_1-X_2-12)^2/120$ are considered where both X_1 and X_2 follow normal distribution with the standard deviation of 0.6. Figure 2 shows the contours of two limit states $G_1=0$ and $G_2=0$ and the corresponding mean value point for X_1 and X_2, which is $d^*=[3.5,3.5]$. The probability of the second-order joint safe event $P(G_1\leq 0,G_2\leq 0)$ stands for the probability that the realized design points are located in region A_1 (feasible region). This probability will be calculated using the CIM at d^*. Based on the procedure of CIM, we define the component events $E_1=\{(X_1,X_2)|G_1\leq 0\}$ and $E_2=\{(X_1,X_2)|G_2\leq 0\}$ and the CI event $E_{12}=\{(X_1,X_2)|G_1\cdot G_2\leq 0\}$. By this definition, $P(E_1)$, $P(E_2)$, and $P(E_{12})$ represent the probabilities of the events that the realized design point will be located in the regions of $A_1\cup A_4$, $A_1\cup A_3$, and $A_3\cup A_4$, respectively. Then, $P(E_1E_2)$, which represents the probability of the second-order joint safe event, can be calculated through the CIM. Table 1 shows the intermediate and final results to calculate the probability of the second-order joint event $P(E_1E_2)$ using Eq. (10). It is noted that compared with MCS results with 1,000,000 sample points, the probabilities of the CI and second-order joint safe events are precisely estimated using the EDR method.

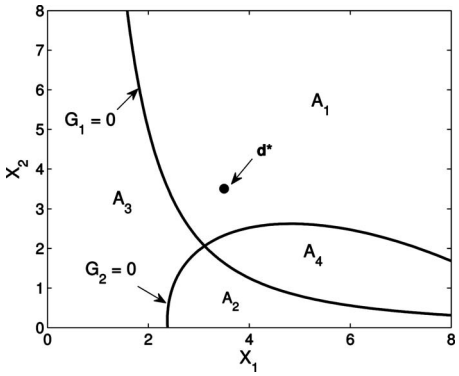

Fig. 2 Mean value point d^* and contours of two limit state functions

Table 1 Procedure and results for probability calculation

Procedure		FORM	SORM	EDR	MCS
Step 1	$P(E_1)$	0.8983	0.8920	0.8813	0.8857
	$P(E_2)$	0.8914	0.8999	0.9150	0.9122
Step 2	$P(E_{12})$	0.0819	0.0986	0.1823	0.1841
Step 3	$P(E_1E_2)$	0.8539	0.8467	0.8070	0.8069

3.2 CI-Matrix. For large-scale systems, the CI events can be conveniently written in the CI-matrix. For instance, if the system includes m components in total, the CI-matrix is defined as

$$\mathrm{CI}=\begin{bmatrix} P(E_1) & P(E_{12}) & P(E_{13}) & \cdots & P(E_{1m}) \\ - & P(E_2) & P(E_{23}) & \cdots & P(E_{2m}) \\ - & - & P(E_3) & \cdots & P(E_{3m}) \\ - & - & - & \ddots & \vdots \\ - & - & - & - & P(E_m) \end{bmatrix} \tag{12}$$

In the upper triangular CI-matrix, the diagonal elements correspond to the component reliabilities (or probabilities of the first-order CI events), and the element on the ith row and the jth column corresponds to the probability of the second-order CI event E_{ij} if $j<i$. The probabilities of the second-order joint safety and failure events in Eqs. (10) and (11) can be evaluated with the probabilities of all CI events that are found from the CI-matrix.

3.3 An Explicit Formula for System Reliability Assessment. Although the second-order system reliability bound method or the LP bound method can generally give fairly narrow system reliability bounds, system reliability is not unique with an explicit formula. This section introduces an explicit formula for system reliability assessment, which is developed based a mathematical inequality equation. In addition to the second-order reliability bound method and LP bound method, this explicit formula can provide an alternative way for system reliability assessment.

Considering a structural serial system with m components, the probability of system failure can be expressed as

$$P_{\mathrm{fs}}=P\left(\bigcup_{i=1}^{m}\bar{E}_i\right) \tag{13}$$

where p_{fs} represents the probability of system failure and $\bar{E}_i$ denotes the failure event of the ith component. Based on the well known Boolean bounds in Eq. (14), the first-order system reliability bound is given in Eq. (15), as shown in the book by Haldar and Mahadevan [12]

$$\max_i(P(\overline{E_i}))\leq P\left(\bigcup_{i=1}^{m}\bar{E}_i\right)\leq\sum_{i=1}^{m}P(\overline{E_i}) \tag{14}$$

$$\max[P(\overline{E_i})]\leq P_{\mathrm{fs}}\leq\min\left[\sum_{i=1}^{m}P(\overline{E_i}),1\right] \tag{15}$$

However, these methods provide wide bounds of system reliability. Thus, the second-order bound method proposed by Ditlevsen and Bjerager [13] in Eq. (16) is widely used because it gives quite narrow bounds of system reliability,

$$P(\overline{E_1})+\sum_{i=2}^{m}\max\left\{\left[P(\overline{E_i})-\sum_{j=1}^{i-1}P(\overline{E_iE_j})\right],0\right\}$$
$$\leq P_{\mathrm{fs}}\leq\min\left\{\left[\sum_{i=1}^{m}P(\overline{E_i})-\sum_{i=2}^{m}\max_{j<i}P(\overline{E_iE_j})\right],1\right\} \tag{16}$$

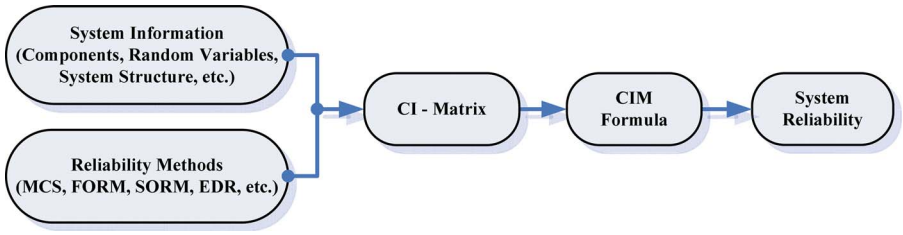

Fig. 3 Flowchart of the CIM for system reliability analysis

where E_1 is the event having the largest probability of failure.

Since the probabilities of all events are non-negative, the following inequalities must be satisfied as

$$\max_i(P(\overline{E_i})) \le \sqrt{\sum_{i=1}^{m}[P(\overline{E_i})]^2} \le \sum_{i=1}^{m} P(\overline{E_i}) \tag{17}$$

First, the left-hand side inequality in Eq. (16) can be redeveloped as

$$P_{\text{fs}} \ge P(\overline{E_1}) + \sum_{i=2}^{m} \max\left\{\left[P(\overline{E_i}) - \sum_{j=1}^{i-1} P(\overline{E_iE_j})\right], 0\right\}$$

$$\ge P(\overline{E_1}) + \sum_{i=2}^{m}\left[P(\overline{E_i}) - \sum_{j=1}^{i-1} P(\overline{E_iE_j})\right] \tag{18}$$

Then, applying the right-hand side inequality in Eq. (17) to Eq. (18) gives the following inequality:

$$P(\overline{E_1}) + \sum_{i=2}^{m}\left[P(\overline{E_i}) - \sum_{j=1}^{i-1} P(\overline{E_iE_j})\right]$$

$$\le P(\overline{E_1}) + \sum_{i=2}^{m}\left\langle P(\overline{E_i}) - \sqrt{\sum_{j=1}^{i-1}[P(\overline{E_iE_j})]^2}\right\rangle \tag{19}$$

where

$$\langle A\rangle \equiv \begin{cases} A & \text{if } A > 0 \\ 0 & \text{if } A \le 0 \end{cases}$$

A similar logic can be applied to the right-hand side inequality in Eq. (16), and it gives

$$P_{\text{fs}} \le \min\left\{\left[\sum_{i=1}^{m} P(\overline{E_i}) - \sum_{i=2}^{m} \max_{j<i} P(\overline{E_iE_j})\right], 1\right\}$$

$$\le \sum_{i=1}^{m} P(\overline{E_i}) - \sum_{i=2}^{m} \max_{j<i} P(\overline{E_iE_j}) \tag{20}$$

Then, using Eqs. (17) and (20) gives

$$\sum_{i=1}^{m} P(\overline{E_i}) - \sum_{i=2}^{m} \max_{j<i} P(\overline{E_iE_j})$$

$$= P(\overline{E_1}) + \sum_{i=2}^{m} P(\overline{E_i}) - \sum_{i=2}^{m} \max_{j<i} P(\overline{E_iE_j})$$

$$\ge P(\overline{E_i}) + \sum_{i=2}^{m}\left\langle P(\overline{E_i}) - \sqrt{\sum_{j=1}^{i-1}[P(\overline{E_iE_j})]^2}\right\rangle \tag{21}$$

The combination of Eqs. (19) and (21) provides the following inequalities:

$$P(\overline{E_1}) + \sum_{i=2}^{m}\left[P(\overline{E_i}) - \sum_{j=1}^{i-1} P(\overline{E_iE_j})\right]$$

$$\le P(\overline{E_1}) + \sum_{i=2}^{m}\left\langle P(\overline{E_i}) - \sqrt{\sum_{j=1}^{i-1}[P(\overline{E_iE_j})]^2}\right\rangle$$

$$\le P(\overline{E_1}) + \sum_{i=2}^{m} P(\overline{E_i}) - \sum_{i=2}^{m} \max_{j<i} P(\overline{E_iE_j}) \tag{22}$$

Finally, Eq. (22) approximates the probability (P_{fs}) of a serial system failure as

$$P_{\text{fs}} \simeq P(\overline{E_1}) + \sum_{i=2}^{m}\left\langle P(\overline{E_i}) - \sqrt{\sum_{j=1}^{i-1}[P(\overline{E_iE_j})]^2}\right\rangle \tag{23}$$

It is proven in Appendix B that this approximate probability lies in the second-order bounds in Eq. (16).

From Eq. (23), the system reliability for a serial system can be assessed as (1—the probability of system failure) and formulated as

$$R_s = P(E_s) \cong P(E_1) - \sum_{i=2}^{m}\left\langle P(\overline{E_i}) - \sqrt{\sum_{j=1}^{i-1}[P(\overline{E_iE_j})]^2}\right\rangle \tag{24}$$

where

$$\langle A\rangle \equiv \begin{cases} A & \text{if } A > 0 \\ 0 & \text{if } A \le 0 \end{cases}$$

Note that the terms inside the bracket, $\langle\ \rangle$, should be ignored if it is less than zero and R_s should be set to zero if the approximated one given by Eq. (24) is less than zero. Equation (24) provides an explicit and unique formula for system reliability assessment based on the second-order reliability bounds shown in Eq. (16) and an inequality of Eq. (17). Although Eq. (24) generally provides better approximation for system reliability, which can be seen from examples shown in Sec. 4, the second-order lower bound can also be used for system-reliability-based design to guarantee a high conservative design. To the application of large system with multiple failure events, The CI-matrix facilitates the evaluation of system reliability. The probability of the CI events can be computed using any reliability analysis method, such as MCS, FORM, SORM, EDR method, and SE methods. Figure 3 shows the procedure for system reliability analysis using the CIM.

4 Results for System Reliability Analysis

This section attempts to check the feasibility of the proposed CIM for system reliability analysis. Three examples, one mathematical example and two practical engineering examples, are used to demonstrate the numerical efficiency and accuracy of the proposed CIM for system reliability analysis. First of all, the CIM, the first-order system reliability bound methods, and the second-

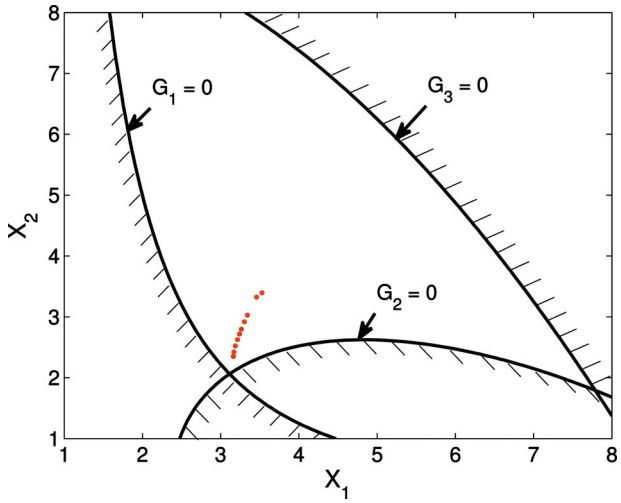

Fig. 4 Three performances in a series system and ten design points

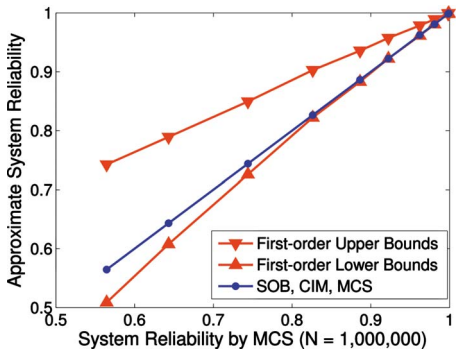

Fig. 5 Accuracy of system reliability analysis at ten design points

order system reliability bound method are employed for system reliability analysis. Their results are compared with those from MCS. This study demonstrates how accurately the CIM estimates system reliability for serial systems. Then, the CI-matrix in the CIM is evaluated using three different reliability methods: FORM, SORM, and the EDR method.

4.1 Mathematical Example. The following mathematical example is used for series system reliability analysis. The series system includes three performances (or responses):

$$G_1(\mathbf{X}) = X_1^2 X_2/20 - 1$$

$$G_2(\mathbf{X}) = (X_1 + X_2 - 5)^2/30 + (X_1 - X_2 - 12)^2/120 - 1$$

$$G_3(\mathbf{X}) = 80/(X_1^2 + 8X_2 + 5) - 1$$

where the random variables, X_1 and X_2, are normally distributed as $X_i \sim N(d_i, 0.3)$, $i=1,2$. Figure 4 gives a schematic view of the component safety and failure events. Three limit state functions ($G_1=0$, $G_2=0$, and $G_3=0$) divide safety events, $E_i=\{(X_1,X_2)|G_i \leq 0\}$ for $i=1-3$, and failure events, $E_i=\{(X_1,X_2)|G_i>0\}$ for $i=1-3$, for three system performances. In this example, system reliabilities will be evaluated at ten different design points dotted in Fig. 4 and listed in Table 2. These ten design points are optimum designs from RBDO using FORM with ten different target reliability levels from 75% to 99.99%.

First, three different system reliability methods are compared with observed mathematical errors in their formulas for system reliability assessment. This study employs the first-order bound method in Eq. (15), the second-order bound method in Eq. (16), and the CIM in Eq. (24). To eliminate numerical errors in system reliability estimates, the MCS with 1,000,000 sample points is employed to evaluate the probabilities of the component safety (or failure), CI, and the second-order joint events required in Eqs. (15), (16), and (24). Results for system reliability assessment are summarized in Table 3. As shown in Fig. 5, the second-order reliability bound method gives unique system reliability instead of a bound. This is because the component reliability for the third component G_3 is so close to 100%. Both the CIM and the second-order system reliability bound method give the identical result to the MCS. However, the first-order system reliability bound method gives wide reliability bounds, especially at relatively low reliability levels.

The study above considers the mathematical error in the different methods for system reliability analysis and found that the CIM and the second-order bound method provide very accurate results, compared with the MCS result. This study attempts to observe numerical error in system reliability that is given by numerically evaluating the system reliability formula of the CIM in Eq. (24). The system reliability formula is numerically computed using three different numerical methods: FORM, SORM, and the EDR method. Again, system reliabilities are evaluated at the ten different designs. The results from FORM, SORM, and the EDR

Table 2 Ten different design points for the mathematical example

Design points	1	2	3	4	5	6	7	8	9	10
d_1	3.1620	3.1694	3.1883	3.2165	3.2413	3.2646	3.3034	3.3411	3.4596	3.5277
d_2	2.3520	2.4239	2.5240	2.6277	2.7187	2.7981	2.9195	3.0274	3.3234	3.3951

Table 3 Results of different system reliability analysis methods for the mathematical example: (1) MCS, (2) first-order bounds (FOBs) using MCS, (3) second-order bounds (SOBs) using MCS, and (4) CIM using MCS (N=1,000,000)

		System reliability at each point									
Analysis methods		1	2	3	4	5	6	7	8	9	10
MCS		0.5645	0.6432	0.7439	0.8263	0.8863	0.9223	0.9622	0.9809	0.9982	0.9991
FOB (MCS)	Lower	0.5088	0.6078	0.7257	0.8221	0.8831	0.9223	0.9614	0.9806	0.9981	0.9991
	Upper	0.7426	0.7892	0.8495	0.9028	0.9028	0.9572	0.9785	0.9892	0.9990	0.9995
SOB (MCS)		0.5645	0.6432	0.7439	0.8263	0.8863	0.9223	0.9622	0.9809	0.9982	0.9991
CIM-MCS		0.5645	0.6432	0.7439	0.8263	0.8863	0.9223	0.9622	0.9809	0.9982	0.9991

Table 4 Results of system reliability analysis using CIM with different numerical reliability methods for the mathematical example: (1) FORM, (2) SORM, and (3) EDR

Methods	System reliability at each point									
	1	2	3	4	5	6	7	8	9	10
MCS (true)	0.5645	0.6432	0.7439	0.8263	0.8863	0.9223	0.9622	0.9809	0.9982	0.9991
CIM_FORM	0.6222	0.7000	0.7908	0.8632	0.9104	0.9404	0.9703	0.9852	0.9985	0.9993
CIM_SORM	0.6062	0.6973	0.7858	0.8594	0.9069	0.9373	0.9680	0.9836	0.9985	0.9992
CIM_EDR	0.5562	0.6357	0.7363	0.8226	0.8823	0.9209	0.9611	0.9804	0.9984	0.9991

method are also compared with those from MCS with 1×10^6 sample points, as shown in Table 4 and Fig. 6. Tables 4 and 5 summarize the result of numerical accuracy and efficiency, respectively. It is found that the EDR method is much more accurate and efficient than MPP-based methods (FORM/SORM) for system reliability assessment because of highly nonlinear behavior of the CI events, which generally require finding multiple MPPs. However, the EDR method calculates the moments of response functions (G_1 or G_2 or G_1*G_2) instead of finding multiple MPPs, which allows the evaluation of the probability of the CI event effectively with no extra effort compared with the evaluation of the probability of the component event. Figure 6 shows relatively higher errors at smaller reliability levels than those at larger reliability levels. It is true no matter what methods are used, except MCS. The error in the CIM comes from the probabilities of the third- or higher-order joint failure events. As the reliability level decreases, the effects of the third- or higher-order joint failure events increase. That is why the error increases as the system reliability decreases. However, the CIM results using the EDR method are least influenced by the reliability levels unlike using FORM or SORM, as shown in Fig. 6. In summary, the CIM using the EDR method appears to be a very accurate and efficient method for system reliability prediction.

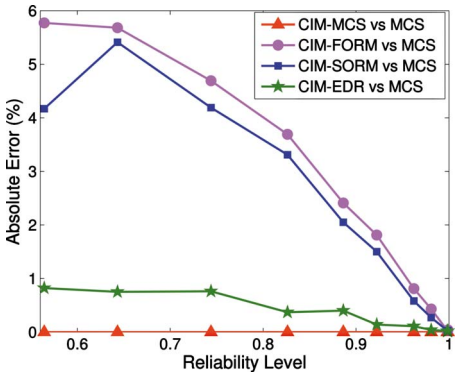

Fig. 6 Absolute errors in system reliability (%) for the mathematical example

Table 5 Efficiency of system reliability analysis using CIM with different numerical reliability methods for the mathematical example: (1) FORM, (2) SORM, and (3) EDR

Methods	EDR	FORM	SORM	MCS
Total number of function evaluation	5	17	17	1,000,000
Total number of sensitivity evaluation	0	17	17	0
Hessian matrix evaluation	0	0	3	0

4.2 Vehicle Side Impact Example. The vehicle side crash analysis example [47] is employed here for system reliability analysis. In this study, the response surfaces for the vehicle side impact (VSI) model (10 constraints and 11 random variables) are employed in this study, and they are found in Appendix B. Random variables and their random properties are summarized in Table 6. System reliability analyses are performed at the eight different design points listed in Table 7. These design points are the optimum designs from RBDO using FORM with eight different target reliability levels. As what has been done in the previous example, the study on mathematical errors in the formula of different system reliability methods is first carried out. Then numerical error is investigated with different numerical methods for reliability assessment.

First, three different system reliability analyses are compared with observed mathematical errors in their formulas for system

Table 6 Properties of random variables in the VSI example

Random variables	Distribution type	Std. dev.
X_1 (B-pillar inner) (mm)	Normal	0.050
X_2 (B-pillar reinforce) (mm)	Normal	0.050
X_3 (floor side inner) (mm)	Lognormal	0.050
X_4 (cross member) (mm)	Lognormal	0.050
X_5 (door beam) (mm)	Uniform	0.050
X_6 (door belt line) (mm)	Uniform	0.050
X_7 (roof rail) (mm)	Uniform	0.050
X_8 (mat. B-pillar inner) (GPa)	Gumbel	0.006
X_9 (mat. Floor side inner) (GPa)	Gumbel	0.006
X_{10} (barrier height) (mm)	Normal	10.00
X_{11} (barrier hitting) (mm)	Normal	10.00

Table 7 Eight different design points for system reliability for the VSI example

Optimum design points	Mean values for random variables										
	X_1	X_2	X_3	X_4	X_5	X_6	X_7	X_8	X_9	X_{10}	X_{11}
1	0.5	1.2669	0.5	1.2298	0.5532	1.5	0.5	0.345	0.1920	0	0
2	0.5	1.2786	0.5	1.2364	0.5680	1.5	0.5	0.345	0.1920	0	0
3	0.5	1.2918	0.5	1.2438	0.5840	1.5	0.5	0.345	0.1920	0	0
4	0.5	1.3071	0.5	1.2524	0.7097	1.5	0.5	0.345	0.1920	0	0
5	0.5	1.3264	0.5	1.2634	0.7389	1.5	0.5	0.345	0.1920	0	0
6	0.5	1.3551	0.5	1.2801	0.8149	1.5	0.5	0.345	0.1920	0	0
7	0.5	1.3876	0.5	1.2998	0.8548	1.5	0.5	0.345	0.1921	0	0
8	0.5	1.4094	0.5	1.3140	0.9945	1.5	0.5003	0.345	0.2511	0	0

Table 8 Results of different system reliability analysis methods for the VSI example: (1) MCS, (2) FOBs using MCS, (3) SOBs using MCS, and (4) CIM using MCS (N=1,000,000)

Methods		System reliability at each point							
		1	2	3	4	5	6	7	8
FOB	Lower	0	0.0961	0.2395	0.4606	0.5867	0.7267	0.8319	0.8748
	Upper	0.4763	0.5269	0.5799	0.6378	0.7055	0.7880	0.8589	0.8937
SOB	Lower	0.2307	0.3036	0.3869	0.5248	0.6225	0.7415	0.8379	0.8812
	Upper	0.2992	0.3491	0.4146	0.5267	0.6235	0.7424	0.8382	0.8822
CIM		0.2511	0.3158	0.3935	0.5257	0.6226	0.7416	0.8379	0.8814
MCS		0.2621	0.3260	0.4017	0.5267	0.6227	0.7417	0.8380	0.8815

reliability assessment. This study employs the first-order bound method in Eq. (15), the second-order bound method in Eq. (16), and the CIM in Eq. (24). To minimize numerical errors in system reliability estimates, the MCS with 1,000,000 sample points is employed to evaluate the probabilities of the component safety (or failure), CI, and the second-order joint events required in Eqs. (15), (16), and (24). Results for system reliability assessment are summarized in Table 8 and graphically shown in Fig. 7. It is found that the second-order bound method gives much narrower bounds than the first-order bound method regardless of the reliability levels. The reliability bounds become narrower as the reliability level increases. In summary, the CIM provides more accurate results at all reliability levels, compared with the first- and second-order bound methods.

Second, this study attempts to observe numerical error in system reliability that is given by numerically evaluating the system reliability formula of the CIM in Eq. (24). The system reliability formula is numerically computed using three different numerical methods: FORM, SORM, and the EDR method. Again, system reliabilities are evaluated at the eight different designs. The results from FORM, SORM, and the EDR method are also compared with those from MCS with 1×10^6 sample points, as shown in Table 9 and Fig. 8. Tables 9 and 10 summarize the result of numerical accuracy and efficiency, respectively. It is also found that the EDR method is much more accurate and efficient than MPP-based methods (FORM/SORM) for system reliability assessment because of the highly nonlinear behavior of the CI events. Again, the CIM results using the EDR method are least influenced by the reliability levels unlike using FORM or SORM, as shown in Fig. 8. The CIM using the EDR method appears to be a very accurate and efficient method for system reliability prediction.

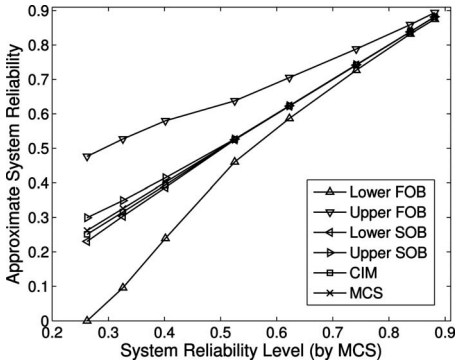

Fig. 7 Accuracy of system reliability analysis at eight design points for the VSI example

4.3 Probabilistic Fatigue Analysis for Large Sea Vessel. Fatigue failure is commonly found in maritime ship structures, and spectral fatigue analyses are often used for predicting the structural lives of maritime ship structures. In this study, fatigue lives of large sea vessel connection ends are considered, and the fatigue system reliability is determined by using CIM with the EDR method. It has been reported that the most critical spot for fatigue failure are longitudinal and transverse connections, as shown in Fig. 9. The finite element (FE) model for this study is shown in Fig. 10 with the model information in Table 11. The end connection in this model is shown in Fig. 11, and in this study four end connections with a total of eight weld hot-spots (each end has one weld heel and weld toe) are considered as a series system, as shown in Fig. 12.

The uncertainties present in this analysis are the loading factors (e.g., wave height and period) and material properties. The variability of the loading factors is accounted for in the development of the stress response spectrum [48]. Even if geometric tolerances are uncertain, small variances in the geometric tolerances of a large vessel will not be a significant contributor to the overall reliability of the welded components. On the other hand, the uncertainties of the signal to noise (S/N) curve can be taken into consideration in the fatigue model after the FE analysis. A total of four parameters of the S/N curve can be considered: c, the S/N curve life intercept; m_1, the negative inverse slope preceding the transition point; m_2, the negative inverse slope following the transition point; and T_p, the location of the transition point. The statistical information of these random variables is located in Table 12. The response value being attained through this fatigue analysis is cumulative fatigue damage ratios, D (=designed life/fatigue life), where the designed life is 20 years. The structure is safe for fatigue when D is less than 1. In order to determine the reliability, the EDR method is used with a $4N+1$ eigenvector samples. Using the EDR method, the CI-matrix is obtained, as shown in Table 12, and accordingly the system reliability for fatigue is obtained through CIM as 0.3877. Based on this calculation, we can also obtain the approximated first-order system reliability bounds as

Table 9 Results of system reliability analysis using CIM with different numerical reliability methods for the VSI example: (1) FORM, (2) SORM, and (3) EDR

Analysis methods	System reliability							
	1	2	3	4	5	6	7	8
CIM-FORM	0.4331	0.5200	0.6370	0.7470	0.8276	0.9177	0.9648	0.9809
CIM-SORM	0.4022	0.4824	0.5721	0.6963	0.7585	0.8581	0.9290	0.9569
CIM-EDR	0.2659	0.3288	0.4013	0.5135	0.6140	0.7253	0.8271	0.8772
MCS	0.2621	0.3260	0.4017	0.5267	0.6227	0.7417	0.8380	0.8815

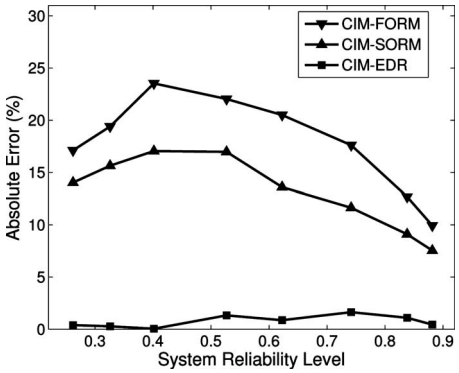

Fig. 8 Absolute errors in system reliability (%) for the VSI example

Table 10 Efficiency of system reliability analysis using CIM with different numerical reliability methods for the VSI example: (1) FORM, (2) SORM, and (3) EDR

Methods	EDR	FORM	SORM	MCS
Total number of function evaluation	23	280	280	1,000,000
Total number of sensitivity evaluation	0	280	280	0
Hessian matrix evaluation	0	0	55	0

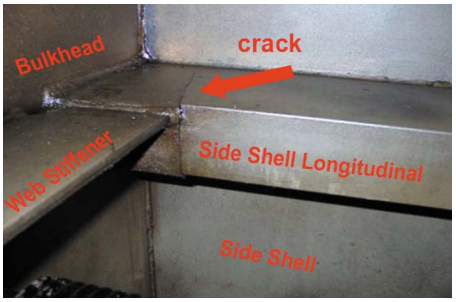

Fig. 9 Sea vessel end connections

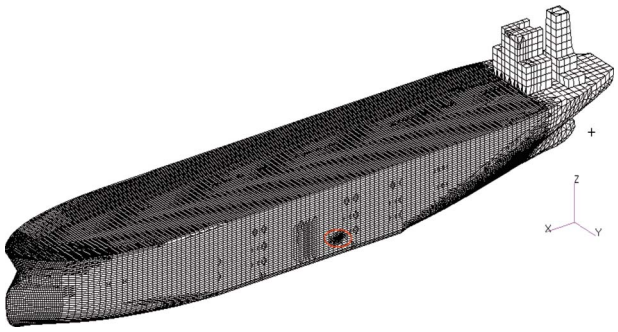

Fig. 10 Sea vessel model

Table 11 Model information (DOF=789,000)

Model component		Amount
Node		131,511
Elements	QUAD4	137,387
	TRIA3	18,959
	BAR	65,697
	ROD	68,157

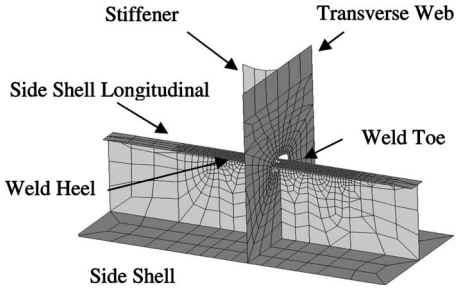

Fig. 11 Longitudinal end connections

$0.3456 \leq R_s \leq 0.3975$. In order to verify the fatigue system reliability result, a MCS is performed using 1000 samples. Both the EDR and MCS results are shown in Table 13. It is found that the EDR method with 17 fatigue analyses gives a good agreement with the MCS in reliability prediction.

5 Conclusion

In this paper, the CIM was proposed to evaluate system reliability for series system. We believe that there are three merits of the proposed method summarized as follows:

(1) Definition of the CI event: The proposed method delivers a unique contribution by defining the CI event. In aid of this definition, the probability of an *N*th-order joint safety event can be decomposed into the probabilities of the first to *N*th-order CI events. As a numerical showcase, the second-order joint safety event can be decomposed into the probabilities of the first- and second-order CI events.
(2) The decomposition of the probabilities of the higher-order joint events: The CIM expresses the probabilities of the second or higher-order joint events analytically in terms of the probabilities of the CI events. With this decomposition, any commonly used numerical reliability methods can be employed for evaluating system reliability.
(3) Numerical solver of the CIM: The EDR method turns out to be more efficient and accurate compared with MPP-based methods mainly due to the highly nonlinear behavior of the CI events. We believe the dimension reduction (DR) family or a polynomial chaos expansion (PCE) will be good candidates for a numerical solver of system reliability.

Furthermore, the CI-matrix facilitates the computation of system reliability for large-scale system applications. In the upper triangular CI-matrix, the diagonal terms are the probabilities of the component safety events (or the first-order CI events), and the off-diagonal terms are the probabilities of the second-order CI events. Two examples were used to demonstrate the effectiveness of the CIM for system reliability assessment in two different ways: (1) with mathematical error and (2) with numerical error and efficiency. First, mathematical errors in the mathematical formula for system reliability were compared among the first- and second-order bound methods and the CIM. It was found that the CIM provides more accurate results at all reliability levels, compared with the first- and second-order bound methods. Second, this study attempted to observe numerical error in system reliability that is given by numerically evaluating the system reliability formula of the CIM. The system reliability formula was numerically computed using three different numerical methods: FORM, SORM, and the EDR method. It is found that the EDR method is much more accurate and efficient than MPP-based methods (FORM/SORM) for system reliability assessment. This is mainly because of the highly nonlinear behavior of the CI events, which generally require finding multiple MPPs. Consequently, the CIM using the EDR method outperforms the existing methods for system reliability prediction in terms of accuracy and efficiency. For

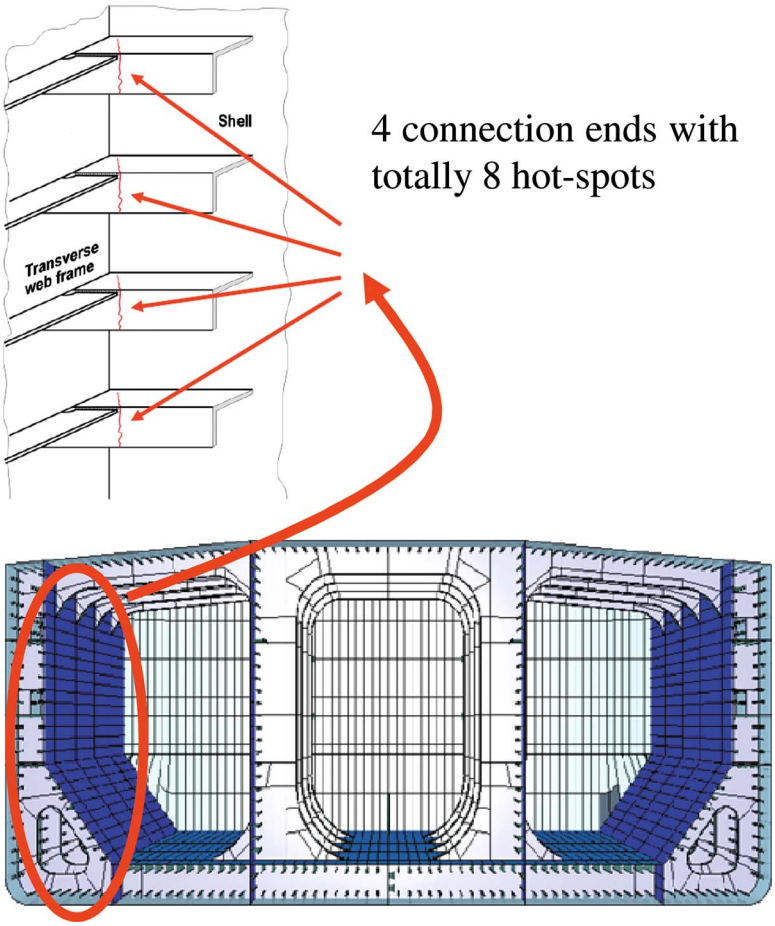

Fig. 12 Definition of system components

Table 12 Statistical parameters of the S/N curve

Variable	c	m_1	m_2	T_p
Distribution	$\sim N(1.52e12, 7.6e10^2)$	$\sim N(3, 0.075^2)$	$\sim N(5, 0.25^2)$	$\sim N(1e7, 5e5^2)$

$$\text{CI (fatigue)} = \begin{bmatrix} 0.3975 & 0.5736 & 0.6093 & 0.6092 & 0.6114 & 0.6090 & 0.5986 & 0.6109 \\ & 0.9564 & 0.0430 & 0.0430 & 0.0419 & 0.0431 & 0.0395 & 0.0421 \\ & & 1 & 1.5\times10^{-6} & 4.7\times10^{-5} & 9.4\times10^{-7} & 0.0085 & 2.2\times10^{-5} \\ & & & 1 & 4.2\times10^{-5} & 6.5\times10^{-7} & 0.0085 & 1.9\times10^{-5} \\ & & & & 0.9999 & 3.5\times10^{-5} & 0.0089 & 0.0001 \\ & & & & & 1 & 0.0084 & 1.6\times10^{-5} \\ & & & & & & 0.9918 & 0.0086 \\ & & & & & & & 1 \end{bmatrix}$$

system-reliability-based design optimization, the explicit and unique formula for system reliability can be used, or alternatively, the second-order lower bound can be used to guarantee a highly conservative design. The CIM will be further investigated for large-scale parallel mixed systems and system-reliability-based design as well.

Table 13 Comparison of results from EDR and MCS

System reliability		Error	Analysis
CIM_EDR	0.3877	1.09%	17
CIM_MCS	0.3960	0.00%	1000
MCS	0.3960	NA	

Acknowledgment

The work presented in this paper has been partially supported by the U.S. National Science Foundation under Grant No. GOALI-07294, by the U.S. Army TARDEC under STAS Contract No. TCN-05122, by General Motors under Grant No. TCS02723, and by FRAMAX Corp. The authors would like to thank Dr. Hong

Table 14 Probability decomposition of the two component system

	CI events		
Basic events	$P(E_1)$	$P(E_2)$	$P(E_{12})$
$P(E_1E_2)$	1	1	0
$P(\bar{E}_1E_2)$	0	1	1
$P(E_1\bar{E}_2)$	1	0	1
$P(\bar{E}_1\bar{E}_2)$	0	0	0

Table 15 Probability decomposition of the two component system with grouping

	CI events	
Basic events	$P(E_1)+P(E_2)$	$P(E_{12})$
$P(E_1E_2)$	2	0
$P(\bar{E}_1E_2)+P(E_1\bar{E}_2)$	1	1
$P(\bar{E}_1\bar{E}_2)$	0	0

Ku Lee from Korea Registry of Shipping for providing the Large Sea Vessel case study.

Nomenclature

- E_i = safe event (or first-order complementary intersection event) of the ith system component
- E_{ij} = complementary intersection event for the ith and jth system components
- E_iE_j = the joint event of the ith and jth system components
- P_f = probability of failure
- Φ = standard Gaussian cumulative distribution function
- $P(E_i)$ = probability of event E_i
- $f_x(x)$ = probability density function
- p_{fs} = probability of system failure
- G_i = function of the ith constraint
- β = reliability index
- κ = principal curvatures

Appendix A: The Derivation of the Decomposition Theorem

Hailperin [49] divided the sample space of a system with N number of the component events into 2^N mutually exclusive and collectively exhaustive (MECE) events, each consisting of a distinct intersection of the component events E_i and their complements $\bar{E}_i$, $i=1,\ldots,N$. They are called the basic events. For example, in the case of three ($=N$) component events, one finds the $2^3=8$ basic events to be $E_1E_2E_3$, $\bar{E}_1E_2E_3$, $E_1\bar{E}_2E_3$, $E_1E_2\bar{E}_3$, $\bar{E}_1\bar{E}_2E_3$, $\bar{E}_1E_2\bar{E}_3$, $E_1\bar{E}_2\bar{E}_3$, and $\bar{E}_1\bar{E}_2\bar{E}_3$. For any system with N number of components, there are 2^N basic events, and any event can be expressed as a linear combination of the basic events. The basic events can be classified into $N+1$ groups where the basic events in the ith group include i number of component failure events:

0th group: $\bigcap_{i=1}^{N} E_i$

1st group: $\bar{E}_j \bigcap_{i=1, i\neq j}^{N} E_i, \quad j=1,2,\ldots,N$

$\vdots \qquad \vdots$

rst group: $\bigcap_{k_1=1}^{N} \bar{E}_{k_j} \bigcap_{\substack{i=1 \\ i\neq k_j}}^{N} E_j, \quad j=1,2,\ldots,r$ with $k_2=k_1+1, \ldots, k_r=k_1+r$

$\vdots \qquad \vdots$

Nth group: $\bigcap_{i=1}^{N} \bar{E}_i$

For example, the basic event in the 0th group, $E_1E_2,\ldots,E_N$ ($\equiv E_1\cap E_2\cap\cdots\cap E_N$), has no component failure event, whereas the basic events ($\bar{E}_1E_2E_3,\ldots,E_N$ and $E_1\bar{E}_2E_3,\ldots,E_N$) in the first group have one component failure event.

The probability of any order CI events can be expressed as a linear combination of the probabilities of the basic events in the $N+1$ group. For the system with two components, the coefficients of the linear combinations are shown in Table 14. For example, the first column of Table 14 can be expressed as

$$P(E_1) = 1\times P(E_1E_2) + 0\times P(\bar{E}_1E_2) + 1\times P(E_1\bar{E}_2) + 0\times P(\bar{E}_1\bar{E}_2)$$
$$= [P(E_1E_2), P(\bar{E}_1E_2), P(E_1\bar{E}_2), P(\bar{E}_1\bar{E}_2\bar{E}_3)] \times [1 \quad 0 \quad 1 \quad 0]^T$$

Grouping the basic events into $N+1$ different groups can give us the compact expression of the linear combinations. Then it is possible to express the summation of the probabilities of the CI events as a linear combination of the probabilities of the basic events in a compact manner. For systems with two components, the coefficients of the linear combinations are shown in Table 15. For example, the first column of Table 15 can be expressed as

$$\sum_{i=1}^{2} P(E_i) = 2\times P(E_1E_2) + 1\times [P(\bar{E}_1E_2) + P(E_1\bar{E}_2)] + 0\times P(\bar{E}_1\bar{E}_2) \tag{A1}$$

Using Table 15, the probability of the second-order joint event can be decomposed into the CI events as

$$P(E_1E_2) = \tfrac{1}{2}[P(E_1) + P(E_2) - P(E_{12})] \tag{A2}$$

Let us consider a general system with N number of the components in total. Table 16 displays a linear combination of the CI events in the general system. For that system, the following equations can be developed for two different cases:

- Case I: N is an odd number,

Table 16 Probability decomposition of the *N* component system

	$P(E_i)$	$P(E_{ij})$	$P(E_{ijk})$	$P(E_{ijkl})$	$P(E_{ijklm})$	$\cdots$	$P(E_{12,\ldots,N})$
$\bigcap_{i=1}^{N} E_i$	C_N^1	0	C_N^3	0	C_N^5	$\cdots$	1, N is odd 0, N is even
$\sum_{j=1}^{N} P(\bigcap_{i=1,i\neq j}^{N} E_i\bar{E}_j)$	C_{N-1}^1	C_{N-1}^1	C_{N-1}^3	C_{N-1}^3	C_{N-1}^5	$\cdots$	0, N is odd 1, N is even
$\sum_{\substack{j=1\\k=2\\j<k}}^{N} P(\bigcap_{\substack{i=1\\i\neq j,k\\j<k}}^{N} E_i\bar{E}_j\bar{E}_k)$	C_{N-2}^1	$2^*C_{N-2}^1$	$C_{N-2}^1+C_{N-2}^3$	$2^*C_{N-2}^3$	$C_{N-2}^3+C_{N-2}^5$	$\cdots$	1, N is odd 0, N is even
$\sum_{\substack{j=1\\k=2\\r=3\\j<k<r}}^{N} P(\bigcap_{\substack{i=1\\i\neq j,k,r}}^{N} E_i\bar{E}_j\bar{E}_k\bar{E}_r)$	C_{N-3}^1	$3^*C_{N-3}^1$	$3^*C_{N-3}^1+C_{N-3}^3$	$C_{N-3}^1+3^*C_{N-3}^3$	$3^*C_{N-3}^3+C_{N-3}^5$	$\cdots$	0, N is odd 1, N is even
$\vdots$	$\vdots$	$\vdots$	$\vdots$	$\vdots$	$\vdots$	$\cdots$	$\vdots$
$P(\bigcap_{i=1}^{N}\bar{E}_i)$	0	0	0	0	0	0	0

$$\sum_{i=1}^{N} P(E_i) - \sum_{\substack{i=1\\j=2\\i<j}}^{N} P(E_{ij}) + \sum_{\substack{i=1\\j=2\\k=3\\i<j<k}}^{N} P(E_{ijk}) + \cdots + (-1)^{m-1} \sum_{\substack{i=1\\j=2\\\vdots\\l=m\\i<j<\cdots<l}}^{N} P(\underbrace{E_{ij\ldots l}}_{m}) + \cdots + (-1)^{N-1} P(E_{12\cdots N})$$

$$= (C_N^1 + C_N^3 + \cdots + C_N^N)\cdot P\left(\bigcap_{i=1}^{N} E_i\right) + (C_{N-1}^1 - C_{N-1}^1 + C_{N-1}^3 - C_{N-1}^3 + \cdots + C_{N-1}^{N-2} - C_{N-1}^{N-2})\cdot \sum_{j=1}^{N} P\left(\bar{E}_j \bigcap_{i=1,i\neq j}^{N} E_i\right)$$

$$+ (C_{N-2}^1 - 2C_{N-2}^1 + C_{N-2}^1 + C_{N-2}^3 - 2^*C_{N-2}^3 + C_{N-2}^3 + C_{N-2}^5 + \cdots)\cdot \sum_{\substack{j=1\\k=2\\j<k}}^{N} P\left(\bar{E}_j\bar{E}_k \bigcap_{\substack{i=1\\i\neq j,k}}^{N} E_i\right) + \cdots + (0-0+0-0+\cdots)P\left(\bigcap_{i=1}^{N}\bar{E}_i\right)$$

$$= 2^{N-1}\cdot P\left(\bigcap_{i=1}^{N} E_i\right)$$

- Case II: N is an even number,

$$\sum_{i=1}^{N} P(E_i) - \sum_{\substack{i=1\\j=2\\i<j}}^{N} P(E_{ij}) + \sum_{\substack{i=1\\j=2\\k=3\\i<j<k}}^{N} P(E_{ijk}) + \cdots + (-1)^{m-1} \sum_{\substack{i=1\\j=2\\\vdots\\l=m\\i<j<\cdots<l}}^{N} P(\underbrace{E_{ij\ldots l}}_{m}) + \cdots + (-1)^{N-1} P(E_{12\cdots N})$$

$$= (C_N^1 + C_N^3 + \cdots + C_N^{N-1})\cdot P\left(\bigcap_{i=1}^{N} E_i\right) + (C_{N-1}^1 - C_{N-1}^1 + C_{N-1}^3 - C_{N-1}^3 + \cdots + C_{N-1}^{N-1} - C_{N-1}^{N-1})\cdot \sum_{j=1}^{N} P\left(\bar{E}_j \bigcap_{i=1,i\neq j}^{N} E_i\right)$$

$$+ (C_{N-2}^1 - 2C_{N-2}^1 + C_{N-2}^1 + C_{N-2}^3 - 2^*C_{N-2}^3 + C_{N-2}^3 + C_{N-2}^5 + \cdots)\cdot \sum_{\substack{j=1\\k=2\\j<k}}^{N} P\left(\bar{E}_j\bar{E}_k \bigcap_{\substack{i=1\\i\neq j\ k}}^{N} E_i\right) + \cdots + (0-0+0-0+\cdots)P\left(\bigcap_{i=1}^{N}\bar{E}_i\right)$$

$$= 2^{N-1}\cdot P\left(\bigcap_{i=1}^{N} E_i\right)$$

From the equations above, the general formula for decomposing the probability of the Nth-order joint event can be developed and expressed as

$$P\left(\bigcap_{i=1}^{N} E_i\right) = \frac{1}{2^{N-1}}\left[\sum_{i=1}^{N} P(E_i) - \sum_{\substack{i=1\\j=2\\i<j}}^{N} P(E_{ij}) + \sum_{\substack{i=1\\j=2\\k=3\\i<j<k}}^{N} P(E_{ijk}) + \cdots + (-1)^{m-1} \sum_{\substack{i=1\\j=2\\\vdots\\l=m\\i<j<\cdots<l}}^{N} P(\underbrace{E_{ij\cdots l}}_{m}) + \cdots + (-1)^{N-1} P(E_{12\cdots N})\right] \tag{A3}$$

Appendix B: Proof

$$P(\overline{E_1}) + \sum_{i=2}^{m} \max\left\{\left[P(\overline{E_i}) - \sum_{j=1}^{i-1} P(\overline{E_i E_j})\right], 0\right\} \le \hat{P}_{\mathrm{fs}} \le \min\left\{\left[\sum_{i=1}^{m} P(\overline{E_i}) - \sum_{i=2}^{m} \max_{j<i} P(\overline{E_i E_j})\right], 1\right\} \tag{B1}$$

where

$$\hat{P}_{\mathrm{fs}} = P(\overline{E_1}) + \sum_{i=2}^{m} \left\langle P(\overline{E_i}) - \sqrt{\sum_{j=1}^{i-1} [P(\overline{E_i E_j})]^2} \right\rangle \tag{B2}$$

and

$$\langle A \rangle \equiv \begin{cases} A & \text{if } A > 0 \\ 0 & \text{if } A \le 0 \end{cases}$$

Proof. From Eq. (17), the following inequality equation holds:

$$\max_i (P(\overline{E_i E_j})) \le \sqrt{\sum_{i=1}^{m} [P(\overline{E_i E_j})]^2} \le \sum_{i=1}^{m} P(\overline{E_i E_j}) \tag{B3}$$

First, consider the inequality between the second-order lower bound and approximated $\hat{P}_{\mathrm{fs}}$. There are two cases:

- Case I:

$$P(\overline{E_i}) \ge \sum_{j=1}^{i-1} P(\overline{E_i E_j})$$

where $i=2,3,\ldots,m$. Then for the second-order lower bound,

$$\max\left\{\left[P(\overline{E_i}) - \sum_{j=1}^{i-1} P(\overline{E_i E_j})\right], 0\right\} = P(\overline{E_i}) - \sum_{j=1}^{i-1} P(\overline{E_i E_j}) \le P(\overline{E_i}) - \sqrt{\sum_{j=1}^{i-1} [P(\overline{E_i E_j})]^2} \tag{B4}$$

- Case II:

$$P(\overline{E_i}) \le \sum_{j=1}^{i-1} P(\overline{E_i E_j})$$

where $i=2,3,\ldots,m$.

If

$$P(\overline{E_i}) \le \sqrt{\sum_{j=1}^{i-1} [P(\overline{E_i E_j})]^2}$$

$$\max\left\{\left[P(\overline{E_i}) - \sum_{j=1}^{i-1} P(\overline{E_i E_j})\right], 0\right\} = \left\langle P(\overline{E_i}) - \sqrt{\sum_{j=1}^{i-1} [P(\overline{E_i E_j})]^2} \right\rangle = 0 \tag{B5}$$

If

$$P(\overline{E_i}) \ge \sqrt{\sum_{j=1}^{i-1} [P(\overline{E_i E_j})]^2}$$

$$\max\left\{\left[P(\overline{E_i}) - \sum_{j=1}^{i-1} P(\overline{E_i E_j})\right], 0\right\} = 0 \le \left\langle P(\overline{E_i}) - \sqrt{\sum_{j=1}^{i-1} [P(\overline{E_i E_j})]^2} \right\rangle \tag{B6}$$

From both Cases I and II, we have

$$\max\left\{\left[P(\overline{E_i}) - \sum_{j=1}^{i-1} P(\overline{E_i E_j})\right], 0\right\} \le \left\langle P(\overline{E_i}) - \sqrt{\sum_{j=1}^{i-1} [P(\overline{E_i E_j})]^2} \right\rangle \tag{B7}$$

Accordingly, we have

$$P(\overline{E_1}) + \sum_{i=2}^{m} \max\left\{\left[P(\overline{E_i}) - \sum_{j=1}^{i-1} P(\overline{E_i E_j})\right], 0\right\} \le P(\overline{E_1}) + \sum_{i=2}^{m} \left\langle P(\overline{E_i}) - \sqrt{\sum_{j=1}^{i-1} [P(\overline{E_i E_j})]^2} \right\rangle \tag{B8}$$

Second, consider the inequality between the second-order upper bound and approximated $\hat{P}_{\mathrm{fs}}$. There are two cases:

- Case I:

$$\sum_{i=1}^{m} P(\overline{E_i}) - \sum_{i=2}^{m} \max_{j<i} P(\overline{E_i E_j}) \le 1$$

Then for the second-order upper bound,

$$\min\left\{\left[\sum_{i=1}^{m} P(\overline{E_i}) - \sum_{i=2}^{m} \max_{j<i} P(\overline{E_i E_j})\right], 1\right\} = \sum_{i=1}^{m} P(\overline{E_i}) - \sum_{i=2}^{m} \max_{j<i} P(\overline{E_i E_j}) = P(\overline{E_1}) + \sum_{i=2}^{m} [P(\overline{E_i}) - \max_{j<i} P(\overline{E_i E_j})]$$

$$\geq P(\overline{E_1}) + \sum_{i=2}^{m}\left[P(\overline{E_i}) - \sqrt{\sum_{j=1}^{i-1}[P(\overline{E_iE_j})]^2}\right] \tag{B9}$$

- Case II:

$$\sum_{i=1}^{m} P(\overline{E_i}) - \sum_{i=2}^{m} \max_{j<i} P(\overline{E_iE_j}) \geq 1$$

If

$$\sum_{i=1}^{m} P(\overline{E_i}) - \sum_{i=2}^{m} \sqrt{\sum_{j=1}^{i-1}[P(\overline{E_iE_j})]^2} \leq 1$$

then for the second-order upper bound,

$$\begin{aligned}\min\left\{\left[\sum_{i=1}^{m} P(\overline{E_i}) - \sum_{i=2}^{m} \max_{j<i} P(\overline{E_iE_j})\right], 1\right\} &\geq \sum_{i=1}^{m} P(\overline{E_i}) - \sum_{i=2}^{m}\left[\sqrt{\sum_{j=1}^{i-1}[P(\overline{E_iE_j})]^2}\right] \\ &= P(\overline{E_1}) + \sum_{i=2}^{m}\left[P(\overline{E_i}) - \sqrt{\sum_{j=1}^{i-1}[P(\overline{E_iE_j})]^2}\right]\end{aligned} \tag{B10}$$

If

$$\sum_{i=1}^{m} P(\overline{E_i}) - \sum_{i=2}^{m} \sqrt{\sum_{j=1}^{i-1}[P(\overline{E_iE_j})]^2} \geq 1$$

$$\min\left\{\left[\sum_{i=1}^{m} P(\overline{E_i}) - \sum_{i=2}^{m} \max_{j<i} P(\overline{E_iE_j})\right], 1\right\} = 1 \tag{B11}$$

$$\begin{aligned}\hat{P}_{\mathrm{fs}} &= P(\overline{E_1}) + \sum_{i=2}^{m}\left[P(\overline{E_i}) - \sqrt{\sum_{j=1}^{i-1}[P(\overline{E_iE_j})]^2}\right] \\ &= \sum_{i=1}^{m} P(\overline{E_i}) - \sum_{i=2}^{m}\left[\sqrt{\sum_{j=1}^{i-1}[P(\overline{E_iE_j})]^2}\right] \geq 1\end{aligned} \tag{B12}$$

Since $\hat{P}_{\mathrm{fs}}$ should always be small or equal to 1, so in this case $\hat{P}_{\mathrm{fs}}$ should be set to 1, which equals to the second-order upper bound.

From both Cases I and II, we have

$$\sum_{i=1}^{m} P(\overline{E_i}) - \sum_{i=2}^{m}\left[\sqrt{\sum_{j=1}^{i-1}[P(\overline{E_iE_j})]^2}\right] \leq \min\left\{\left[\sum_{i=1}^{m} P(\overline{E_i}) - \sum_{i=2}^{m} \max_{j<i} P(\overline{E_iE_j})\right], 1\right\} \tag{B13}$$

Finally, the combination of Eqs. (A8) and (A13) gives the desired result. ■

Appendix C: Response Surface of Vehicle Side Impact Model

The response surface for ten constraints of the vehicle side impact model is constructed as $\{G_i < g_i,\ i=1,2,\ldots,10\}$ where g_i are from vector $g=[1,32,32,32,0.32,0.32,0.32,4,9.9,15.7]$ and G_i are as follows:

$$G_1 = 1.16 - 0.3717X_2X_4 - 0.00931X_2X_{10} - 0.484X_3X_9 + 0.01343X_6X_{10}$$

$$G_2 = 28.98 + 3.818X_3 - 4.2X_1X_2 + 0.0207X_5X_{10} + 6.63X_6X_9 - 7.7X_7X_8 + 0.32X_9X_{10}$$

$$G_3 = 33.86 + 2.95X_3 + 0.1792X_{10} - 5.057X_1X_2 - 11X_2X_8 - 0.0215X_5X_{10} - 9.98X_7X_8 + 22X_8X_9$$

$$G_4 = 46.36 - 9.9X_2 - 12.9X_1X_8 + 0.1107X_3X_{10}$$

$$G_5 = 0.261 - 0.0159X_1X_2 - 0.188X_1X_8 - 0.019X_2X_7 + 0.0144X_3X_5 + 0.0008757X_5X_{10} + 0.08045X_6X_9 + 0.00139X_8X_{11} + 0.00001575X_{10}X_{11}$$

$$G_6 = 0.214 + 0.00817X_5 - 0.131X_1X_8 - 0.0704X_1X_9 + 0.03099X_2X_6 - 0.018X_2X_7 + 0.0208X_3X_8 + 0.121X_3X_9 - 0.00364X_5X_6 + 0.0007715X_5X_{10} - 0.0005354X_6X_{10} + 0.00121X_8X_{11} + 0.00184X_9X_{10} - 0.018X_2^2$$

$$G_7 = 0.74 - 0.61x_2 - 0.163X_3X_8 + 0.001232X_3X_{10} - 0.166X_7X_9 + 0.227X_2^2$$

$$G_8 = 4.72 - 0.5X_4 - 0.19X_2X_3 - 0.0122X_4X_{10} + 0.009325X_6X_{10} + 0.000191X_{11}^2$$

$$G_9 = 10.58 - 0.674X_1X_2 - 1.95X_2X_8 + 0.02054X_3X_{10} - 0.0198X_4X_{10} + 0.028X_6X_{10}$$

$$G_{10} = 16.45 - 0.489X_3X_7 - 0.843X_5X_6 + 0.0432X_9X_{10} - 0.0556X_9X_{11} - 0.000786X_{11}^2$$

References

[1] Du, X., and Chen, W., 2004, "Sequential Optimization and Reliability Assessment Method for Efficient Probabilistic Design," ASME J. Mech. Des., **126**(2), pp. 225–233.

[2] Youn, B. D., Choi, K. K., and Du, L., 2005, "Enriched Performance Measure Approach (PMA+) for Reliability-Based Design Optimization," AIAA J., **43**(4), pp. 874–884.

[3] McDonald, M., and Mahadevan, S., 2008, "Reliability-Based Optimization With Discrete and Continuous Decision and Random Variables," ASME J. Mech. Des., **130**(6), p. 061401.

[4] Kim, C., and Choi, K. K., 2008, "Reliability-Based Design Optimization Using Response Surface Method With Prediction Interval Estimation," ASME J. Mech. Des., **130**(12), p. 121401.

[5] Zou, T., Mourelatos, Z. P., and Mahadevan, S., 2008, "An Indicator Response Surface Method for Simulation-Based Reliability Analysis," ASME J. Mech. Des., **130**(7), p. 071401.

[6] Youn, B. D., Choi, K. K., and Du, L., 2005, "Adaptive Probability Analysis Using An Enhanced Hybrid Mean Value (HMV+) Method," Struct. Multidiscip. Optim., **29**(2), pp. 134–148.

[7] Du, X., Sudjianto, A., and Chen, W., 2004, "An Integrated Framework for Optimization Under Uncertainty Using Inverse Reliability Strategy," ASME J. Mech. Des., **126**(4), pp. 562–764.

[8] Rahman, S., and Xu, H., 2004, "A Univariate Dimension-Reduction Method for Multi-Dimensional Integration in Stochastic Mechanics," Probab. Eng. Mech., **19**, pp. 393–408.

[9] Youn, B. D., Xi, Z., and Wang, P. F., 2008, "Eigenvector Dimension-Reduction (EDR) Method for Derivative-Free Uncertainty Quantification," Struct. Multidiscip. Optim., **37**(1), pp. 13–28.

[10] Ang, A. H.-S., and Amin, M., 1967, "Studies of Probabilistic Safety Analysis of Structures and Structural Systems," University of Illinois, Urbana.

[11] Bennett, R. M., and Ang, A. H.-S., "Investigation of Methods for Structural System Reliability," Ph.D. thesis, University of Illinois, Urbana.

[12] Haldar, A., and Mahadevan, S., 2000, *Probability, Reliability, and Statistical Methods in Engineering Design*, Wiley, New York, pp. 238–248.

[13] Ditlevsen, O., and Bjerager, P., 1984, "Narrow Reliability Bounds for Structural Systems," J. Eng. Mech., **110**(5), pp. 671–693.

[14] Thoft-Christensen, P., and Murotsu, Y., 1986, *Application of Structural Reliability Theory*, Springer, Berlin.

[15] Karamchandani, A., 1987, "Structural System Reliability Analysis Methods," John A. Blume Earthquake Engineering Center, Stanford University, Report No. 83.

[16] Xiao, Q., and Mahadevan, S., 1998, "Second-Order Upper Bounds on Probability of Intersection of Failure Events," J. Eng. Mech., **120**(3), pp. 49–57.
[17] Ramachandran, K., 2004, "System Reliability Bounds: A New Look With Improvements," Civ. Eng. Environ. Syst., **21**(4), pp. 265–278.
[18] Song, J., and Der Kiureghian, A., 2003, "Bounds on System Reliability by Linear Programming," J. Eng. Mech. **129**(6), pp. 627–636.
[19] Royset, J., Der Kiureghian, A., and Polak, E., 2001, "Reliability-Based Optimal Design of Series Structural Systems," J. Eng. Mech., **127**(6), pp. 607–614.
[20] Zou, T., and Mahadevan, S., 2006, "A Direct Decoupling Approach for Efficient Reliability Based Design Optimization," Struct. Multidiscip. Optim., **31**(3), pp. 190–200.
[21] Liang, J., Mourelatos, Z. P., and Nikolaidis, E., 2007, "A Single-Loop Approach for System Reliability-Based Design Optimization," ASME J. Mech. Des., **129**(12), pp. 1215–1224.
[22] McDonald, M., and Mahadevan, S., 2008, "Design Optimization With System-Level Reliability Constraints," ASME J. Mech. Des., **130**(2), p. 021403.
[23] Mahadevan, S., and Raghothamachar, P., 2000, "Adaptive Simulation for System Reliability Analysis of Large Structures," Comput. Struct., **77**, pp. 725–734.
[24] Zou, T., and Mahadevan, S., 2006, "Versatile Formulation for Multi-Objective Reliability-Based Design Optimization," ASME J. Mech. Des., **128**, pp. 1217–1226.
[25] Zhou, L., Penmetsa, R. C., and Grandhi, R. V., 2000, "Structural System Reliability Prediction Using Multi-Point Approximations for Design," Eighth ASCE Specialty Conference on Probabilistic Mechanics and Structural Reliability, Paper No. PMC2000-082.
[26] Sues, R. H., and Cesare, M. A., 2005, "System Reliability and Sensitivity Factors via the MPPSS Method," Probab. Eng. Mech., **20**, pp. 148–157.
[27] Niederreiter, H., and Spanier, J., 2000, *Monte Carlo and Quasi-Monte Carlo Methods*, Springer, Berlin.
[28] Bucher, C. G., 1988, "Adaptive Sampling—An Iterative Fast Monte Carlo Procedure," Struct. Safety, **5**, pp. 119–126.
[29] Wu, Y.-T., 1994, "Computational Methods for Efficient Structural Reliability and Reliability Sensitivity Analysis," AIAA J., **32**(8), pp. 1717–1723.
[30] Bjerager, P., 1988, "Probability Integration by Directional Simulation," J. Eng. Mech., **114**, pp. 1285–1302.
[31] Hohenbichler, M., and Rackwitz, R., 1983, "First-Order Concepts in System Reliability," Struct. Safety, **1**, pp. 177–188.
[32] Kleiber, M., and Hien, T. D., 1992, *The Stochastic Finite Element Method*, Wiley, New York.
[33] Rahman, S., and Rao, B. N., 2001, "A Perturbation Method for Stochastic Meshless Analysis in Elastostatics," Int. J. Numer. Methods Eng., **50**, pp. 1969–1991.
[34] Yamazaki, F., and Shinozuka, M., 1988, "Neumann Expansion for Stochastic Finite Element Analysis," J. Eng. Mech., **114**, pp. 1335–1354.
[35] Hasofer, A. M., and Lind, N. C., 1974, "Exact and Invariant Second-Moment Code Format," J. Eng. Mech., **100**, pp. 111–121.
[36] Wu, Y. T., Millwater, H. R., and Cruse, T. A., 1990, "Advanced Probabilistic Structural Analysis Method for Implicit Performance Functions," AIAA J., **28**(9), pp. 1663–1669.
[37] Du, X., and Chen, W., 2004, "Sequential Optimization and Reliability Assessment Method for Efficient Probabilistic Design," ASME J. Mech. Des., **126**(2), pp. 225–233.
[38] Du, X., 2008, "Unified Uncertainty Analysis by the First Order Reliability Method," ASME J. Mech. Des., **130**(9), p. 091401.
[39] Lee, S. H., and Kwak, B. M., 2006, "Response Surface Augmented Moment Method for Efficient Reliability Analysis," Struct. Safety, **28**, pp. 261–272.
[40] Xu, H., and Rahman, S., 2004, "A Generalized Dimension-Reduction Method for Multidimensional Integration in Stochastic Mechanics," Int. J. Numer. Methods Eng., **61**, pp. 1992–2019.
[41] Yuan, X.-X., and Pandey, M. D., 2006, "Analysis of Approximations for Multinormal Integration in System Reliability Computation," Struct. Safety, **28**, pp. 361–377.
[42] Zhao, Y. G., and Ono, T., 2001, "Moment Methods for Structural Reliability," Struct. Safety, **23**, pp. 47–75.
[43] Choi, S.-K., Grandhi, R. V., and Canfied, R. A., 2007, *Reliability-Based Structural Design*, Springer, London.
[44] Youn, B. D., and Choi, K. K., 2004, "A New Response Surface Methodology for Reliability Based Design Optimization," Comput. Struct., **82**, pp. 241–256.
[45] Myers, R. H., and Montgomery, D. C., 1995, *Response Surface Methodology: Process and Product in Optimization Using Designed Experiments*, Wiley, New York.
[46] Johnson, N. L., Kotz, S., and Balakrishnan, N., 1995, *Continuous Univariate Distributions*, Wiley, New York.
[47] Youn, B. D., Choi, K. K., Gu, L., and Yang, R.-J., 2004, "Reliability-Based Design Optimization for Crashworthiness of Side Impact," Struct. Multidiscip. Optim., **26**(3–4), pp. 272–283.
[48] Youn, B. D., Wells, L. J., and Lee, H. K., 2007, "Probabilistic Fatigue Analysis Using the Eigenvector Dimension Reduction (EDR) Method," WCSMO, Seoul, Korea, Paper No. A0181.
[49] Hailperin, T., 1965, "Best Possible Inequalities for the Probability of a Logical Function of Events," Am. Math. Monthly, **72**(4), pp. 343–359.